



Published in final edited form as:

Science. 2016 April 22; 352(6284): 463–466. doi:10.1126/science.aaf3926.

## Mx1 reveals innate pathways to antiviral resistance and lethal influenza disease

Padmini S. Pillai<sup>1</sup>, Ryan D. Molony<sup>1</sup>, Kimberly Martinod<sup>2</sup>, Huiping Dong<sup>1</sup>, Iris K. Pang<sup>1</sup>, Michal C. Tal<sup>1,\*</sup>, Angel G. Solis<sup>1</sup>, Piotr Bielecki<sup>1</sup>, Subhasis Mohanty<sup>3</sup>, Mark Trentalange<sup>4</sup>, Robert J. Homer<sup>5</sup>, Richard A. Flavell<sup>1,8</sup>, Denisa D. Wagner<sup>2</sup>, Ruth R. Montgomery<sup>6</sup>, Albert C. Shaw<sup>3</sup>, Peter Staeheli<sup>7</sup>, and Akiko Iwasaki<sup>1,8,†</sup>

<sup>1</sup>Department of Immunobiology, Yale School of Medicine, New Haven, CT 06520, USA

<sup>2</sup>Program in Cellular and Molecular Medicine, Boston Children's Hospital, Harvard Medical School, Boston, MA, USA

<sup>3</sup>Section of Infectious Diseases, Department of Internal Medicine, Yale School of Medicine, New Haven, Connecticut, USA

<sup>4</sup>Department of Internal Medicine, Yale School of Medicine, New Haven, Connecticut, USA

<sup>5</sup>Department of Pathology, Yale School of Medicine, New Haven, CT 06520, USA

<sup>6</sup>Section of Rheumatology, Department of Internal Medicine, Yale School of Medicine, New Haven, CT 06520, USA

<sup>7</sup>Institut für Medizinische Mikrobiologie und Hygiene, Institute of Virology, University Medical Center Freiburg, Hermann-Herder-Strasse 11, 79104 Freiburg, Germany

<sup>8</sup>Howard Hughes Medical Institute, Yale School of Medicine, New Haven, CT 06520, USA

### Abstract

Influenza A virus (IAV) causes up to half a million deaths worldwide annually, 90% of which occur in older adults. We show that IAV-infected monocytes from older humans have impaired antiviral interferon production but retain intact inflammasome responses. To understand the in vivo consequence, we used mice expressing a functional *Mx* gene encoding a major interferon-induced effector against IAV in humans. In *Mx1*-intact mice with weakened resistance due to deficiencies in *Mavs* and *Tlr7*, we found an elevated respiratory bacterial burden. Notably, mortality in the absence of *Mavs* and *Tlr7* was independent of viral load or MyD88-dependent signaling but dependent on bacterial burden, caspase-1/11, and neutrophil-dependent tissue damage. Therefore, in the context of weakened antiviral resistance, vulnerability to IAV disease is a function of caspase-dependent pathology.

<sup>†</sup>Corresponding author. akiko.iwasaki@yale.edu.

Present address: Institute of Stem Cell Biology and Regenerative Medicine, School of Medicine, Stanford, CA 94305, USA.

#### SUPPLEMENTARY MATERIALS

[www.sciencemag.org/content/352/6284/463/suppl/DC1](http://www.sciencemag.org/content/352/6284/463/suppl/DC1)) Materials and Methods

Table S1

Figs. S1 to S11

References (36–47)

Respiratory infections with influenza A virus (IAV) cause severe morbidity and mortality in humans and animals worldwide. Older humans are highly susceptible to influenza disease. This susceptibility could be due to an inability to mount an effective antiviral response or an incapacity to develop disease tolerance to IAV infection (1–4). We began by comparing the innate immune pathways engaged by IAV infections in peripheral blood monocytes from young-adult (20- to 30-year-old) and older (65- to 89-year-old) human donors (table S1 and fig. S1A). IAV-infected monocytes from older humans showed intact nuclear factor  $\kappa$ B (NF- $\kappa$ B)-dependent proinflammatory cytokine expression and secretion [interleukin (IL)- $\delta$ ] (fig. S1B and Fig. 1A) and robust inflammasome-dependent cytokine expression and secretion (IL-1 $\beta$ ) (fig. S1C and Fig. 1B). Type I interferon (IFN) responses to IAV infection, however, were significantly attenuated in older human monocytes (IFN- $\beta$ ) (Fig. 1C). Reduced IFN secretion from older monocytes was not attributable to the expression level of RIG-I, a viral RNA sensor that induces the type I IFN responses that drive antiviral immunity (5, 6) (fig. S1D) or to a particular demographic group (fig. S1, E to G). Similar age-dependent reduction in IFN- $\beta$  was observed from monocytes transfected with ligands of RIG-I (fig. S2, A to F) and from macrophages stimulated with polyinosinic-polycytidylic acid (fig. S2, G to I). These data indicate that older human monocytes and macrophages have intact RIG-I signaling to activate proinflammatory cytokines and the inflammasome but have impaired signaling to induce type I IFNs.

Comparison of a broader array of genes revealed that infected monocytes from older donors showed consistently lower expression of several IFN-stimulated genes (ISGs) (MxA, IFITM2, and ISG15, all of which are known to have antiviral activities for influenza viruses) (Fig. 1D). Furthermore, expression of IRF7, a critical transcription factor for type I IFNs, and STAT1, a type I IFN receptor signaling molecule, was lower in the older cohort. Consequently, older monocytes infected with IAV expressed higher levels of influenza viral genes (NS and M) (Fig. 1D). Selective impairment in IFN responses to other viral infections (7), after vaccination against influenza (8) or downstream of TLR7 (4,9,10), suggest that decreased IFN and elevated proinflammatory cytokines are a common characteristic of the aging innate immune system in humans.

To probe the possible in vivo consequences of weak IFN responses in the face of robust inflammation after IAV infection, we sought to employ a relevant mouse model. Older C57BL/6 mice did not show increased susceptibility to IAV infection over young mice; in fact, older mice showed antiviral resistance (fig. S3), failing to phenocopy aging human infections (11). We therefore decided to mimic human innate effector responses using genetic approaches to determine the consequences of the loss of pattern recognition receptors (PRRs) that induce IFNs during IAV infection. Inbred mouse strains, including C57BL/6, carry nonfunctional alleles of the *Mx1* gene. The myxovirus resistance protein 1 (Mx1) is a dynamin-like guanosine triphosphatase that blocks primary transcription of influenza, presumably by binding to viral nucleoproteins (12–14). We predicted that intact Mx1 would affect the dynamics of viral spread and the host response to IAV infection, and that *Mx1*-sufficient mice would more closely model influenza pathogenesis in humans. As reported previously (15,16), Mx1 congenic mice on the C57BL/6 background were highly resistant to IAV (A/PR8) infections as compared with Mx1-deficient C57BL/6 mice (fig. S4). The observed resistance in Mx1 congenic mice was not due to more robust adaptive

immunity because these mice showed low levels of T and B cell-mediated responses to IAV, likely because of rapid viral clearance (fig. S4, D and E).

We therefore used Mx1 mice to investigate the relative contributions of the innate immune-sensing pathways during IAV infection: Toll-like receptors (TLRs) and RIG-I, which both induce type I IFNs (5), and the inflammasome pathway that activates caspase-1, releases IL-1 $\beta$  and IL-18, and induces pyroptosis (17,18). At a high dose of viral challenge [10<sup>6</sup> plaque-forming units (PFU)], *Tlr7*<sup>-/-</sup> or *Casp1/11*<sup>-/-</sup> mice survived infection, whereas *Mavs*<sup>-/-</sup> and *Tlr7*<sup>-/-</sup>  $\times$  *Mavs*<sup>-/-</sup> mice lost weight and died by day 7 or day 5, respectively, with a high viral burden (fig. S5). After challenge with a lower dose of A/PR8 virus (100 PFU), *Tlr7*<sup>-/-</sup>, *Mavs*<sup>-/-</sup>, and *Casp1/11*<sup>-/-</sup> mice were resistant, but *Tlr7*<sup>-/-</sup>  $\times$  *Mavs*<sup>-/-</sup> double-deficient mice lost weight and succumbed to infection (Fig. 2, A and B). The mechanism of protection conferred by MAVS and TLR7 in the *Mx1*-sufficient host correlated with the ability of these PRRs to induce IFN- $\beta$  secretion (Fig. 2C). In contrast, inflammatory cytokine secretion was observed independently of MAVS and TLR7 (fig. S6). Mice deficient in both *Mavs* and *Tlr7* lost Mx1 expression (Fig. 2D and fig. S7) and therefore succumbed to IAV challenge. Thus, unlike C57BL/6 mice (19–22), Mx1 congenic mice reveal the key innate sensors that confer antiviral resistance, RIG-I and TLR7; these sensors are responsible for the production of type I IFNs that induce Mx1 expression and potentially control IAV replication. This is consistent with our results in monocytes from older humans, where impaired RIG-I signaling led to low IFN induction and compromised innate IAV resistance (Fig. 1).

To assess the role of inflammasome activation in the context of an impaired interferon response, we generated Mx1 congenic *Tlr7*<sup>-/-</sup>  $\times$  *Mavs*<sup>-/-</sup>  $\times$  *Casp1/11*<sup>-/-</sup> mice. Strikingly, these mice exhibited protection from IAV disease (Fig. 3, A and B) despite having viral loads similar to *Tlr7*<sup>-/-</sup>  $\times$  *Mavs*<sup>-/-</sup> mice (Fig. 3C and fig. S8A). Improved protection was therefore not a function of greater antiviral resistance but a lack of *Casp1/11* activity. *Tlr7*<sup>-/-</sup>  $\times$  *Mavs*<sup>-/-</sup>  $\times$  *Casp1/11*<sup>-/-</sup> mice eventually cleared the virus by 30 days after infection (fig. S8B). *Tlr7*<sup>-/-</sup>  $\times$  *Mavs*<sup>-/-</sup> mice also succumbed to infection with a human isolate of the 2009 pandemic strain of H1N1 (pH1N1) faster than other genotypes at two challenge doses (fig. S9). Furthermore, *Tlr7*<sup>-/-</sup>  $\times$  *Mavs*<sup>-/-</sup>  $\times$  *Casp1/11*<sup>-/-</sup> mice exhibited longer survival compared with *Tlr7*<sup>-/-</sup>  $\times$  *Mavs*<sup>-/-</sup> mice at a challenge dose of 10<sup>5</sup> PFU (fig. S9, C and D). These results indicate that after IAV infection, *Casp1/11* deficiency confers a survival advantage in the context of combined *Tlr7* and *Mavs* deficiency.

Next, we investigated the contributions of caspase-1/11 -dependent cytokines, IL-1 $\beta$  and IL-18, in driving IAV disease and lethality. MyD88 is an adaptor protein required for signaling downstream of IL-1R and IL-18R (23), as well as TLR7. Unlike *Tlr7*<sup>-/-</sup>  $\times$  *Mavs*<sup>-/-</sup>  $\times$  *Casp1/11*<sup>-/-</sup> mice, Mx1 congenic *MyD88*<sup>-/-</sup>  $\times$  *Mavs*<sup>-/-</sup> mice succumbed to A/PR8 infection, albeit with a delayed time course compared with *Tlr7*<sup>-/-</sup>  $\times$  *Mavs*<sup>-/-</sup> mice (Fig. 3D). Infected *MyD88*<sup>-/-</sup>  $\times$  *Mavs*<sup>-/-</sup> mice sustained levels of IAV burden in the lung similar to *Tlr7*<sup>-/-</sup>  $\times$  *Mavs*<sup>-/-</sup> and *Tlr7*<sup>-/-</sup>  $\times$  *Mavs*<sup>-/-</sup>  $\times$  *Casp1/11*<sup>-/-</sup> mice (fig. S8B). In addition, treatment with Anakinra (IL-1R antagonist) failed to rescue *Tlr7*<sup>-/-</sup>  $\times$  *Mavs*<sup>-/-</sup> mice from IAV-induced lethality (Fig. 3D). Histological analysis of the lungs (fig. S10) revealed that *Tlr7*<sup>-/-</sup>  $\times$  *Mavs*<sup>-/-</sup> mice sustained severe inflammation around airways and suffered from

airway degeneration and epithelial and venular necrosis (fig. S10B, arrow). In contrast, *Tlr7<sup>-/-</sup> × Mavs<sup>-/-</sup> × Casp1/11<sup>-/-</sup>* mice had less severe inflammation and reduced venular necrosis. Therefore, signaling through IL-1R and IL-18R is insufficient to drive IAV-induced mortality in the absence of RLR and TLR signaling, and a separate function of caspase-1/11, leading to inflammation and tissue damage, is required for lethal disease after IAV infection.

One of the hallmarks of caspase-1/11 activation is the recruitment of neutrophils (24). Neutrophilic infiltration largely accounts for fatal influenza gene signatures (25). Robust and comparable recruitment of many inflammatory leukocytes, including neutrophils, was observed in both *Tlr7<sup>-/-</sup> × Mavs<sup>-/-</sup>* and *Tlr7<sup>-/-</sup> × Mavs<sup>-/-</sup> × Casp1/11<sup>-/-</sup>* mice infected with IAV (fig. S11). To determine whether neutrophils mediate disease and lethality in *Tlr7<sup>-/-</sup> × Mavs<sup>-/-</sup>* mice carrying functional *Mx1* alleles, we depleted neutrophils in vivo using an antibody to Ly6G. Half of neutrophil-depleted *Tlr7<sup>-/-</sup> × Mavs<sup>-/-</sup>* mice survived the infection (Fig. 4A), indicating that neutrophils contribute to IAV lethality. Neutrophils mediate clearance of bacteria and fungi but also cause immunopathology, owing to their release of reactive oxygen species and neutrophil extracellular traps (NETs) (26). Notably, the lungs of the IAV-infected *Tlr7<sup>-/-</sup> × Mavs<sup>-/-</sup>* mice had significantly higher staining for NETs (27) than the *Tlr7<sup>-/-</sup> × Mavs<sup>-/-</sup> × Casp1/11<sup>-/-</sup>* mice (Fig. 4B and fig. S12). Furthermore, we found that caspase-1/11 was also required for NET formation in the lung after intranasal inoculation of bacterial lipopolysaccharide (LPS) (fig. S13), indicating that the requirement of *Casp1/11* for NET release extends beyond IAV infection. NET digestion by treatment with deoxyribonuclease (DNase) (Pulmozyme) resulted in prolonged survival of *Tlr7<sup>-/-</sup> × Mavs<sup>-/-</sup>* mice after IAV infection (Fig. 4A). Thus, in the absence of *Tlr7* and *Mavs*, NETosis contributes to mortality after IAV infection, likely in part by inducing collateral tissue damage (28). Despite the lack of innate viral control, depletion of neutrophils or degradation of NETs can induce disease tolerance to influenza.

Older adults (>65 years of age) are most vulnerable to the flu, and many succumb to pneumonia caused by secondary bacterial infections (29, 30). IAV infection and consequent airway epithelial damage are sufficient to enhance bacterial colonization of the lungs (31–35). Therefore, we hypothesized that IAV-induced disease and mortality in the *Tlr7<sup>-/-</sup> × Mavs<sup>-/-</sup>* mice may be secondary to bacterial infection. Notably, bacterial bloom was observed in the nasal cavity of infected *Tlr7<sup>-/-</sup> × Mavs<sup>-/-</sup>* and *Tlr7<sup>-/-</sup> × Mavs<sup>-/-</sup> × Casp1/11<sup>-/-</sup>* mice, as compared with the IAV-resistant wild-type mice (Fig. 4, C and D). In addition, an increase in the abundance of *Pasteurellaceae* was observed in the nasal cavities (Fig. 4E) and lungs (Fig. 4, F and G) of IAV-infected *Tlr7<sup>-/-</sup> × Mavs<sup>-/-</sup>* and *Tlr7<sup>-/-</sup> × Mavs<sup>-/-</sup> × Casp1/11<sup>-/-</sup>* mice. Finally, combination antibiotic treatment beginning 3 days after IAV infection partially rescued *Tlr7<sup>-/-</sup> × Mavs<sup>-/-</sup>* mice from lethality (Fig. 4H). Collectively, these data indicate that a failure to induce type I IFNs promotes viral amplification and tissue damage within the respiratory environment, conducive to bacterial bloom. Neutrophil recruitment and caspase-dependent NETosis contributes to lethality. These results in *Mx1* congenic mice are consistent with the notion that age-related defects in innate immunity (reduced IFN responses) could predispose IAV-infected older adults to secondary bacterial infection. A direct implication of our findings is that older adults suffering from IAV infection may benefit from therapeutic strategies that minimize inflammatory responses mediated by neutrophils.

## Supplementary Material

Refer to Web version on PubMed Central for supplementary material.

## Acknowledgments

The data presented in this manuscript are tabulated in the main paper and in the supplementary materials. Sequence data has been publicly released to the general scientific community (NCBI Sequence Read Archive ID SRR3216492). This study was supported by NIH awards AI081884, AI062428, and AI064705 (to A.I.); HHSN272201100019C (to A.C.S. and R. R. M.); K24 AG02489 (to A.C.S.); T32 AI007019-36 (to P.S.P.); T32 AI007019-38 and T32 AI055403 (to R.D.M.); 5T32HL066987-13 (to K.M.); F31 AG039163 (to M.T.); R01HL102101 and R01HL125501 (to D.D.W.); K24 AG042489 (to A.C.S.); P30 AG21342 (Claude D. Pepper Older Americans Independence Center at Yale) (to A.C.S.); and grant SFB1160/P13 from the Deutsche Forschungsgemeinschaft (DFG) (to P.S.). A.I. and R.A.F. are investigators of the Howard Hughes Medical Institute.

## REFERENCES AND NOTES

1. Ayres JS, Schneider DS. *Annu Rev Immunol.* 2012; 30:271–294. [PubMed: 22224770]
2. Medzhitov R, Schneider DS, Soares MP. *Science.* 2012; 335:936–941. [PubMed: 22363001]
3. Råberg L, Sim D, Read AF. *Science.* 2007; 318:812–814. [PubMed: 17975068]
4. Shaw AC, Goldstein DR, Montgomery RR. *Nat Rev Immunol.* 2013; 13:875–887. [PubMed: 24157572]
5. Taniguchi T, Takaoka A. *Curr Opin Immunol.* 2002; 14:111–116. [PubMed: 11790540]
6. Vela A, Fedorova O, Ding SC, Pyle AM. *J Biol Chem.* 2012; 287:42564–42573. [PubMed: 23055530]
7. Qian F, et al. *J Infect Dis.* 2011; 203:1415–1424. [PubMed: 21398396]
8. Mohanty S, et al. *J Infect Dis.* 2015; 211:1174–1184. [PubMed: 25367297]
9. Canaday DH, et al. *J Clin Immunol.* 2010; 30:373–383. [PubMed: 20182777]
10. Sridharan A, et al. *Age (Dordr).* 2011; 33:363–376. [PubMed: 20953722]
11. Vanhooren V, Libert C. *Ageing Res Rev.* 2013; 12:8–21. [PubMed: 22543101]
12. Staeheli P, Haller O, Boll W, Lindenmann J, Weissmann C. *Cell.* 1986; 44:147–158. [PubMed: 3000619]
13. Haller O, Staeheli P, Schwemmle M, Kochs G. *Trends Microbiol.* 2015; 23:154–163. [PubMed: 25572883]
14. Staeheli P, Grob R, Meier E, Sutcliffe JG, Haller O. *Mol Cell Biol.* 1988; 8:4518–4523. [PubMed: 2903437]
15. Kaminski MM, Ohnemus A, Cornitescu M, Staeheli P. *J Gen Virol.* 2012; 93:555–559. [PubMed: 22170637]
16. Moritoh K, et al. *Jpn J Vet Res.* 2009; 57:89–99. [PubMed: 19827744]
17. McAuley JL, et al. *PLOS Pathog.* 2013; 9:e1003392. [PubMed: 23737748]
18. Ichinohe T, Pang IK, Iwasaki A. *Nat Immunol.* 2010; 11:404–410. [PubMed: 20383149]
19. Koyama S, et al. *J Immunol.* 2007; 179:4711–4720. [PubMed: 17878370]
20. Le Goffic R, et al. *PLOS Pathog.* 2006; 2:e53. [PubMed: 16789835]
21. Pang IK, Pillai PS, Iwasaki A. *Proc Natl Acad Sci USA.* 2013; 110:13910–13915. [PubMed: 23918369]
22. Seo SU, et al. *J Virol.* 2010; 84:12713–12722. [PubMed: 20943980]
23. Adachi O, et al. *Immunity.* 1998; 9:143–150. [PubMed: 9697844]
24. Dinarello CA. *Eur J Immunol.* 2011; 41:1203–1217. [PubMed: 21523780]
25. Brandes M, Klauschen F, Kuchen S, Germain RN. *Cell.* 2013; 154:197–212. [PubMed: 23827683]
26. Yipp BG, Kubers P. *Blood.* 2013; 122:2784–2794. [PubMed: 24009232]
27. Brill A, et al. *J Thromb Haemost.* 2012; 10:136–144. [PubMed: 22044575]
28. Saffarzadeh M, et al. *PLOS ONE.* 2012; 7:e32366. [PubMed: 22389696]

29. Thompson WW, et al. *JAMA*. 2003; 289:179–186. [PubMed: 12517228]
30. Medina RA, García-Sastre A. *Nat Rev Microbiol*. 2011; 9:590–603. [PubMed: 21747392]
31. McCullers JA. *Nat Rev Microbiol*. 2014; 12:252–262. [PubMed: 24590244]
32. Pittet LA, Hall-Stoodley L, Rutkowski MR, Harmsen AG. *Am J Respir Cell Mol Biol*. 2010; 42:450–460. [PubMed: 19520922]
33. Siegel SJ, Roche AM, Weiser JN. *Cell Host Microbe*. 2014; 16:55–67. [PubMed: 25011108]
34. Mina MJ, McCullers JA, Klugman KP. *MBio*. 2014; 5:e01040–13. [PubMed: 24549845]
35. McCullers JA, et al. *J Infect Dis*. 2010; 202:1287–1295. [PubMed: 20822454]

Author Manuscript

Author Manuscript

Author Manuscript

Author Manuscript

### Editor's Summary

#### Flu immunity shows its age

As we age, our immune systems change; in many ways not for the better. For instance, the elderly account for 90% of influenza deaths annually. Pillai *et al*, now report that influenza-infected human monocytes, a type of immune cell, exhibit reduced antiviral activity. In influenza-infected mice, two innate immune sensing pathways work together to promote antiviral immunity to influenza. Mice lacking antiviral immunity (similar to the situation in elderly people) had elevated bacterial burdens in their lungs and increased inflammatory responses, which both contributed to their increased susceptibility to influenza.

Author Manuscript

Author Manuscript

Author Manuscript

Author Manuscript

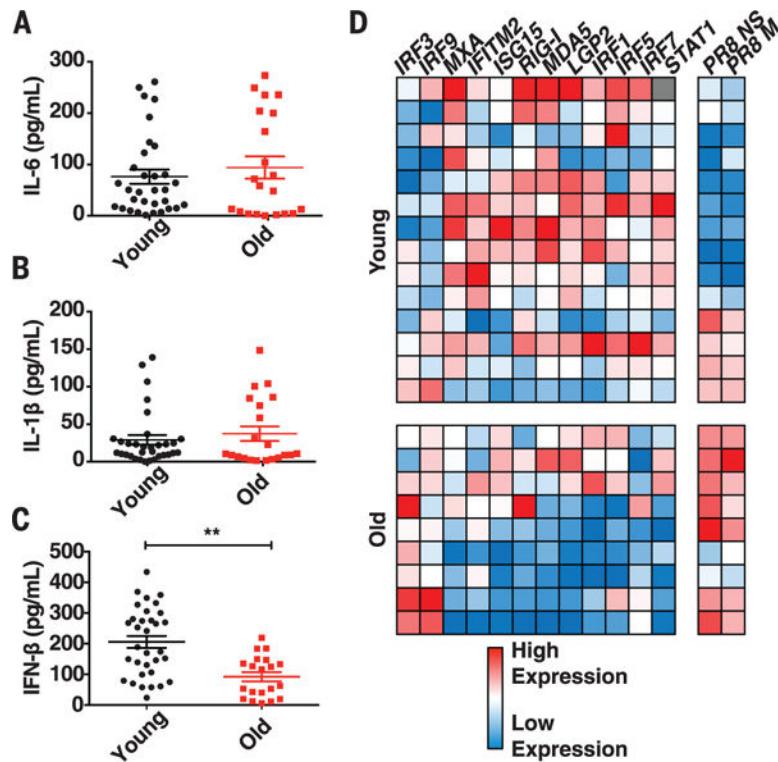


**Fig. 1. Monocytes from old humans have impaired IFN but otherwise intact cytokine responses** Human monocytes from young (age 20 to 30 years;  $n = 33$ ) or old (age 65 to 89 years;  $n = 20$ ) healthy donors were infected with A/PR/8/34 influenza virus at a multiplicity of infection of 10 for 12 hours, after which cell supernatants were collected and analyzed by enzyme-linked immunosorbent assay (ELISA) to measure (A) IL-6, (B) IL-1 $\beta$ , and (C) IFN- $\beta$ . Data are pooled from two independent experiments and are presented as means  $\pm$  SEM. (D) RNA was isolated from PR8-infected monocytes and was analyzed by quantitative polymerase chain reaction (qPCR) to measure relative gene expression. Gene expression data were arranged in a heat map to identify age-related defects. \*\* $P < 0.01$ ; linear mixed-effects models adjusted for covariates,  $P$  values from the post hoc  $t$  statistics are Hochberg adjusted.



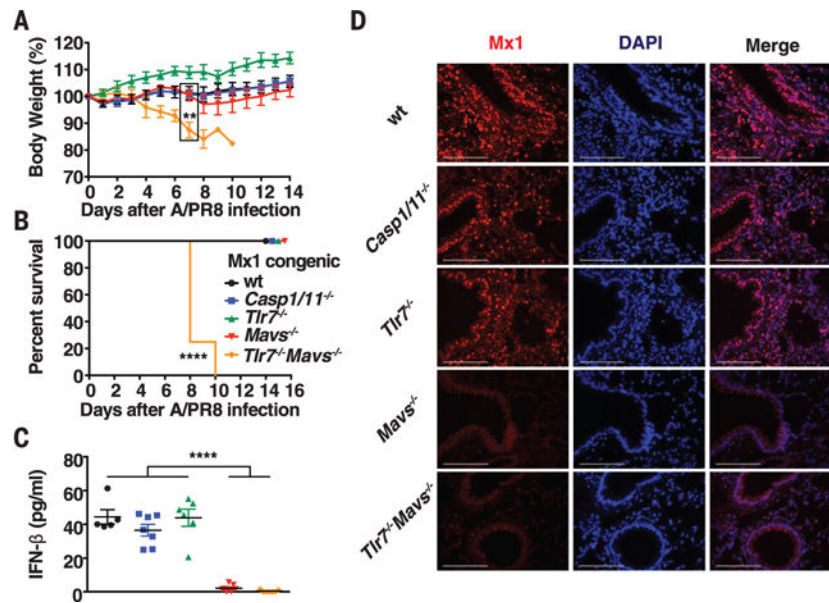


**Fig. 2. RLR and TLR7 induce Mx1 expression and protection after influenza A virus infection** Wild-type, *Casp1/11*<sup>-/-</sup>, *Tlr7*<sup>-/-</sup>, *Mavs*<sup>-/-</sup>, and *Tlr7*<sup>-/-</sup>*Mavs*<sup>-/-</sup> mice carrying functional *Mx1* alleles were infected intranasally (i.n.) with 100 PFU of influenza virus A/PR/8/34. (A) Weight loss and (B) survival were monitored for 14 days ( $n = 5$  to 9 mice per group). (C) Broncho-alveolar lavage (BAL) was collected 48 hours after infection ( $n = 5$  to 7 mice per group), and levels of IFN- $\beta$  were measured by ELISA. Data are means  $\pm$  SEM. (D) Mice were sacrificed on day 2 and lungs were fixed in 4% paraformaldehyde. Tissue was embedded in paraffin, sectioned for staining with a rabbit antibody to mouse Mx1, and visualized by fluorescence microscopy [red, Mx1; blue, counter-staining of nuclei with 4', 6-diamidino-2-phenylindole (DAPI)]. Samples are representative of 3 to 5 mice per group. \*\*\*\* $P < 0.0001$ ; \*\* $P < 0.01$ ; one-way analysis of variance (ANOVA); log-rank (Mantel-Cox).

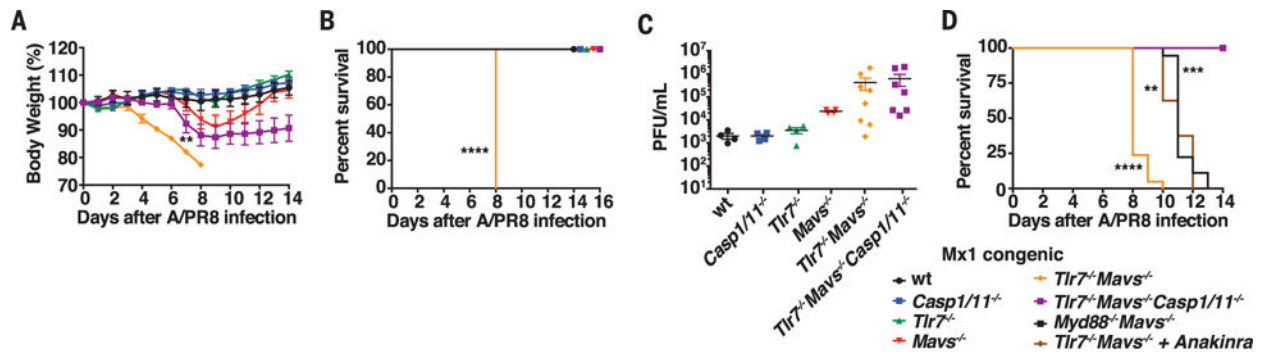


**Fig. 3. In the absence of TLR7 and MAVS, deletion of *Casp1/11* rescues mice from lethality after influenza A virus infection**

Wild-type, *Casp1/11*<sup>-/-</sup>, *Tlr7*<sup>-/-</sup>, *Mavs*<sup>-/-</sup>, *Tlr7*<sup>-/-</sup>*Mavs*<sup>-/-</sup>, and *Tlr7*<sup>-/-</sup>*Mavs*<sup>-/-</sup>*Casp1/11*<sup>-/-</sup> mice carrying functional *Mx1* alleles were infected (i.n.) with 100 PFU of influenza virus A/PR/8/34. (A) Weight loss and (B) survival were monitored for 14 or 16 days, respectively ( $n = 4$  to 10 mice per group). (C) BAL was collected and viral titer was measured ( $n = 4$  to 8 mice per group) on day 4 after infection. Data are means  $\pm$  SEM. (D) *Tlr7*<sup>-/-</sup>*Mavs*<sup>-/-</sup> ( $n = 21$ ), *Tlr7*<sup>-/-</sup>*Mavs*<sup>-/-</sup>*Casp1/11*<sup>-/-</sup> ( $n = 4$ ), and *Myd88*<sup>-/-</sup>*Mavs*<sup>-/-</sup> ( $n = 18$ ) mice carrying functional *Mx1* alleles were infected (i.n.) with 100 PFU of A/PR/8/34 influenza virus. A separate group of *Tlr7*<sup>-/-</sup>*Mavs*<sup>-/-</sup> ( $n = 8$ ) was treated with 100 mg/kg of Anakinra intraperitoneally every 12 hours starting on day -1. Survival was monitored for 2 weeks after infection. Data are pooled from two separate experiments. \*\*\*\* $P < 0.0001$ ; \*\*\* $P < 0.001$ ; \*\* $P < 0.01$ ; one-way ANOVA; log-rank (Mantel-Cox).

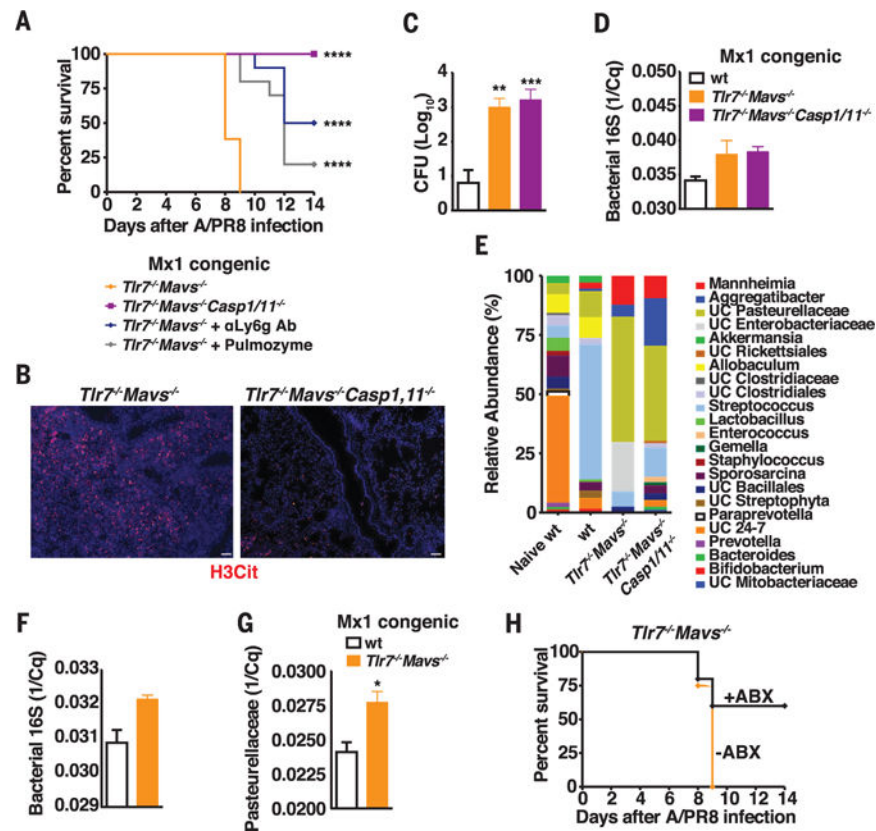


**Fig. 4. Failure to induce type I IFNs and viral control is sufficient to promote bacterial bloom in the lung**

(A) Mice carrying functional *Mx1* alleles were infected (i.n.) with 100 PFU of influenza virus A/PR/8/34. A group of *Tlr7*<sup>-/-</sup>*Mavs*<sup>-/-</sup> mice was treated with either a neutrophil-depleting antibody to Ly6G or recombinant DNase (Pulmozyme) intraperitoneally, daily starting on day -1. Survival was monitored for 14 days ( $n = 8$  to 13 mice per group). (B) Lungs were harvested on day 8, stained with a rabbit antibody to histone H3 (citrulline R2 + R8 + R17) and visualized by fluorescence microscopy (red, H3Cit; blue, counter-staining of nuclei with DAPI). Samples are representative of 3 to 6 samples per group. (C to E) Nasal wash samples collected on day 8 were (C) plated to determine bacterial load and (D) analyzed by qPCR for relative expression levels of 16S rDNA ( $n = 4$  to 5 per group). Data are means  $\pm$  SEM. (E) The average relative abundance of bacterial genera of greater than 1% abundance from naïve wild-type ( $n = 3$ ), wild-type ( $n = 1$ ), *Tlr7*<sup>-/-</sup> *Mavs*<sup>-/-</sup> ( $n = 5$ ), and *Tlr7*<sup>-/-</sup> *Mavs*<sup>-/-</sup> *Casp1/11*<sup>-/-</sup> ( $n = 5$ ) was determined by 16S sequencing. (F and G) After infection with 1000 PFU of PR8, lungs were harvested on day 7 and analyzed by qPCR for relative expression levels of (F) 16S rDNA and (G) bacteria from the *Pasteurellaceae* family ( $n = 3$  to 4 per group). (H) A group of *Tlr7*<sup>-/-</sup>*Mavs*<sup>-/-</sup> mice infected with 100 PFU was administered antibiotics daily by intragastric gavage on days 3 to 10 after infection. Survival was monitored ( $n = 4$  to 5 per group). Data are representative of two similar experiments. \*\*\*\* $P < 0.0001$ ; \*\*\* $P < 0.001$ ; \*\* $P < 0.01$ ; \* $P < 0.05$ ; one-way ANOVA; log-rank (Mantel-Cox).